Available online at www.sciencedirect.com

ScienceDirect

Procedia Engineering 186 (2017) 635 – 642

Procedia Engineering

www.elsevier.com/locate/procedia

18th Conference on Water Distribution System Analysis, WDSA 2016

Hydraulic modelling for pressure reducing valve controller design addressing disturbance rejection and stability properties

Tomasz Janus*, Bogumil Ulanicki

De Montfort University, The Gateway, LE1 9BH, Leicester, United Kingdom

Abstract

Pressure reducing valves (PRVs) are widely used in water distribution systems to reduce excess pressure caused by variations in terrain elevation or by excessive pumping. The fundamental role of a PRV is to maintain a desired outlet pressure irrespectively of hydraulic conditions in the water distribution network (WDN). Unfortunately, even a stable PRV can exhibit poor disturbance rejection resulting in variations of outlet pressure around the setpoint due to randomly varying demands. The aim of this paper is to better understand this phenomenon and to develop models which would facilitate designing effective controllers considering the stability and disturbance rejection issues.

Peer-review under responsibility of the organizing committee of the XVIII International Conference on Water Distribution Systems

Keywords: pressure reducing valve (PRV), stability, disturbance rejection, controller design

1. Introduction

After a number conversations with practitioners and researchers working on pressure management in water distribution networks (WDNs) we have noticed that there seems to be a misconception regarding the cause of occasional oscillations observed in pressure reducing valves (PRVs). This so-called 'hunting' is often attributed to the occurrence of pressure waves which affect pressure readings (in case of electronically controlled valves) causing large temporal variations in controller error and thus, control action. Although such behaviour can in principle be reduced, if not eliminated, by e.g. window averaging of PRV outlet pressure readings and by specifying lower and upper bounds on the control signal, we have found that the main cause of valve instability lies in the intrinsic property of the valve rather than in the hydraulic conditions inside the network. As described in Ulanicki and Skworcow[1] PRVs tend to oscillate under low flow conditions because their dynamic gain decreases nonlinearly with opening. Hence, PRVs have higher gain for lower valve openings than higher ones. Oscillations in valve position can cause significant transients if the opening and closing rate of the control element is sufficiently large. Transients thus seem to be more of a result of PRV instability rather than the cause of it.

Even with the stability issue properly addressed, PRV outlet pressure can still vary around the set-point during normal operation. This variability in the outlet pressure of typically ±(2-3) m H_2O is mainly due to random changes

*Tomasz Janus. Tel.: +44-116-257-7070
E-mail address: tjanus@dmu.ac.uk

1877-7058
Peer-review under responsibility of the organizing committee of the XVIII International Conference on Water Distribution Systems
doi:10.1016/j.proeng.2017.03.280

in water demand across the network, which from the point of view of the controller, is considered a disturbance. Since demand patterns, similarly to instability, also have a periodic character, usually on more than one time scale, it is often difficult to an untrained eye, looking at just pressure measurements, to classify the cause of pressure oscillations as either a PRV instability problem or a lack of disturbance rejection problem. Although the dynamics of PRVs [2] and PRV control systems [3] are now better understood, we are still faced with a number of unanswered questions which need to be addressed in order to improve the robustness, stability, and disturbance rejection within PRVs.

Firstly, we would like to find out whether under normal operating conditions water compressibility and pipe elasticity play any noticeable role in the dynamics of the PRV-WDN system or whether the above effects can be omitted in the model without any significant impairment of accuracy. If the latter is true, the hydraulic equations can be reduced to an incompressible flow problem also known as rigid column. Thus, distributed partial differential network equations are simplified into a lumped ordinary differential equation (ODE) model which allows us to carry out a formal analysis using system and control theory, to ultimately gain a deeper understanding of the performance and the stability of the closed-loop PRV-WDN system. If it turns out that the rigid column model is sufficiently accurate for some operating conditions, we need to determine whether this statement is also true for other operating conditions and draw bounds within which such an assumption is valid. For example, it is very likely that in most industrial applications where actuators are designed such that the rate of valve opening and closure is limited in order to reduce the risk of transients, rigid column approach will yield satisfactorily accurate results whilst in case where the valve is designed to change the control element faster than the travel time of the pressure wave along the pipeline, pressure transients may need to be included in the model.

Second, it is important to understand the interactions between the PRV and other components of a WDN. Specifically, we are interested in understanding how network size and topology affect the stability of the closed-loop PRV-WDN system and how changes in water demands affect the PRV outlet pressure. Whilst the first problem is concerned with system stability the second one addresses the problem of disturbance rejection.

Finally, mathematical analysis of a closed-loop PRV-WDN system prompted a re-examination of the concept of demand-driven WDN simulation from the PRV control perspective. Numerous publications, i.e. Jung et al.[4] already questioned the correctness of a demand-driven approach by providing the evidence that demand-driven simulations in which the flow in the network nodes is forced and thus, is independent from the nodal pressures, overestimates the magnitude and the duration of pressure waves. On the contrary, head-driven simulations in which water demand is pressure-dependent and hence a result of nodal pressures, tend to give more accurate predictions. There are additional implications of fixing demands independently of pressure which shall be discussed, from the control point of view, in Section 4.

2. Model structure

Since the main purpose of this paper is to gain a deeper understanding of the operation of PRVs, not WDNs in general, the network model has been reduced to the upstream and downstream feed pipe only. The rest of the network, shown in dotted lines in Fig. 1, was not modelled. Instead, demands in all major nodes were summed up and total demand was ‘simulated’ at the end of the downstream pipe at node 4 (see Fig. 1). As our hydraulic model is pressure-driven not demand-driven, for the reasons mentioned in Section 1 and later explained in Section 4, demand flow Q is a function of pressure head at node 4 (H_4) and modelled with Toricelli’s orifice equation: $Q(t) = A_{orifice}(t)\ \sqrt{2\,g\ (H_4(t) - z_4)}$ in which z_4 denotes the elevation of node 4 and g is the gravitational constant. The true demand flow pattern is thus approximated with time-dependent total orifice surface area $A_{orifice}(t)$.

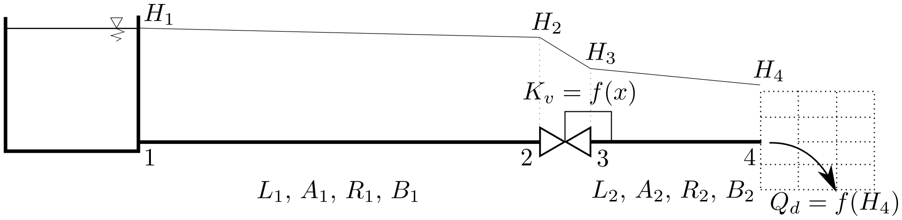

Fig. 1: Schematic of the hydraulic model used for the simulations of the PRV under different operating conditions and network properties.

The PRV-WDN control loop structure and the parameters were borrowed from an industrial case study. The valve with a known capacity characteristic $K_v = K_v(x)$, where x (%) denotes the valve opening, is controlled with a digital PID controller with the following gains: proportional gain $K_p = 0.5$, integral gain $K_i = 0.05$ (i.e. integral time $T_i = 10$s), derivative gain $K_d = 0$; sampling time = 0.1s and hardware gain $K_{hw} = 0.8\%/\text{m}$. The actuator is modelled as a first order system with the time constant of 0.1s. The valve opening and closing rate is limited at $\pm$ 100/87 %/s to reduce the risk of transients. The rate-limited actuator output is then quantized with an interval of 0.5% and goes through a backlash block with a deadband of 0.8%. The pressure drop across the PRV is a function of flow and valve position: $\Delta H_{PRV} = \frac{Q\,|Q|}{[K_v(x)]^2}$. The controller error e is the difference between the downstream head setpoint $H_{out}^{PRV,setpoint}$=106.5m and the downstream pressure measurement $H_{out}^{PRV,ave}$(m) averaged using a moving average filter with a buffer size of 300 data points updated every 0.02s and followed by a zero-order-hold of 0.1s. To reduce the amount of control effort the control system is only active when $|e| \geq 0.5$m, i.e. the outlet head H_{out}^{PRV} is allowed to vary ±0.5m H_2O.

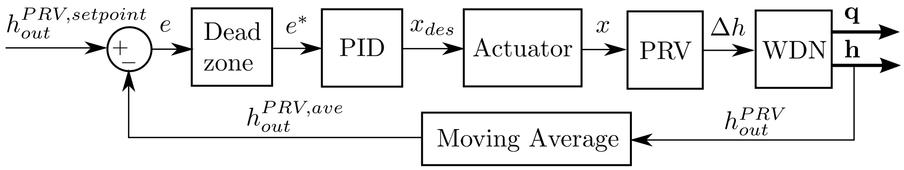

Fig. 2: PRV-WDN closed-loop model structure

3. Model equations

This paper investigates two hydraulic models of an unsteady flow in WDNs: the water-hammer model which considers water compressibility and pipe elasticity effects and the rigid column which assumes that the fluid is incompressible and the conduit is perfectly rigid. The reason for considering the rigid column model is that unlike the water-hammer model it is an ODE system and thus it can be used for controller design whilst the control theory based on distributed partial differential equation (PDE) models such as the water-hammer model has not yet been developed.

3.1. Water-hammer model

The water-hammer model is composed of two hyperbolic PDEs: the continuity equation (Eq. 1) and the momentum equation (Eq. 2) in which H = piezometric head, Q = flow rate, D = pipe diameter, A = pipe cross-section area, λ = the Darcy-Weisbach friction coefficient and θ is the inclination of the pipe. These two equations describe the propagation of pressure waves along a pipe as a response to changing boundary conditions, i.e. pressures and flows at both ends of the pipe. The waves propagate at a constant speed (a) which depends on the pipe's Young's modulus of elasticity (E), pipe wall thickness (e), the fluid density (ρ), and the fluid's bulk modulus of elasticity (K) - see Eq. 3.

$$\frac{\partial H}{\partial t} + \frac{a^2}{g\,A}\frac{\partial Q}{\partial x} = 0 \tag{1}$$

$$\frac{\partial Q}{\partial t} + g\,A\,\frac{\partial H}{\partial x} + g\,A\,\sin\theta + \frac{\lambda\,Q\,|Q|}{2\,D\,A} = 0 \tag{2}$$

$$a = \sqrt{\frac{K}{\rho\left(1 + \frac{D\,K}{e\,E}\right)}} \tag{3}$$

The water-hammer equations are often solved with a method of characteristics which transforms the original two PDEs into two ODEs which are solved for each internal point along the length of the pipe, i.e. $\forall i \in \{2, .., n-1\}$, where n is the number of nodes in the conduit. In a short form these two ODEs can be written as two characteristic equations: $C^+ : \; H_i = C_{p,i} - B\,q_i$ and $C^- : \; H_i = C_{m,i} + B\,q_i$. where $C_{p,i} = H_{i-1}^* + B\,q_{i-1}^* - R\,q_{i-1}^*\left|q_{i-1}^*\right|$ and $C_{m,i} = H_{i+1}^* - B\,q_{i+1}^* + R\,q_{i+1}^*\left|q_{i+1}^*\right|$ in which $B = \dfrac{a}{g\,A}$ and $R = \dfrac{\lambda\,\Delta x}{2\,g\,D\,A^2}$, Δx is the distance between the internal pipe nodes and * denotes the value of the variable recorded in the previous time step.

3.2. Rigid column model

If the boundary conditions are changing slowly enough that the amount of stress exerted on the pipe walls and the fluid itself is insufficient to cause any significant deformation of the pipe and the fluid, we can treat the problem as incompressible flow in a rigid conduit. For such a flow type $E = \infty$ and $K = \infty$ and hence, accordingly to Eq. 3, pressure wave speed $a = \infty$. The changes in pressure boundary conditions thus propagate instantly along the entire network. The flow of incompressible fluid in a rigid conduit is described with Eq. 2 in which partial derivatives have been replaced with ordinary derivative terms.

$$\frac{dQ}{dt} + g\,A\,\frac{dH}{dx} + g\,A\,\sin\theta + \frac{\lambda\,Q\,|Q|}{2\,D\,A} = 0 \tag{4}$$

After integrating Eq. 4 over the length of the upstream and downstream pipe (see Fig. 1), eliminating the $g\,A\sin\theta$ term since it has been assumed that $\theta = 0$, and adding the two pipe equations together, we obtained the following rigid-column model.

$$\frac{dQ}{dt}\,(J_1 + J_2) = H_1 - (R_1 + R_2)\;Q\,|Q| - \frac{Q\,|Q|}{[K_v(x)]^2} - H_4 \tag{5}$$

where $J_1 = \frac{L_1}{g\,A_1}$, $J_2 = \frac{L_2}{g\,A_2}$ are two inertial terms and L_1, A_1, L_2, A_2 are the lengths and cross-section areas of upstream and downstream pipes. In a pressure-driven flow configuration, where the outlet flow is a function downstream head (H_4), H_4 in Eq. 5 is a function of Q and $A_{orifice}$ - see Section 2 for details.

3.3. Initial and boundary conditions

The initial flow value Q_0 is obtained from Eq. 5 for $\frac{dQ}{dt} = 0$ with inputs $A_{orifice}(t = 0) = A_{orifice,0}$ and $x(t = 0) = x_0$. Next, the piezometric head values are calculated for nodes 2, 3, and 4 with static equations of fluid flow. In the water-hammer model, all nodal flow values are assigned the initial flow value Q_0, i.e. $\forall i \in \{1, .., n\}: \; Q_i = Q_0$. The internal head values H_i are obtained through a linear interpolation between the boundary head values. The boundary conditions for the water-hammer model are listed in Table 1. Both pipes combined are discretized into $n-1$ segments, in which node m represents node 2 in the rigid column model, node $m + 1$ = node 3, whilst node n represents node 4.

Table 1: Boundary conditions for the water-hammer model.

Upstream reservoir	PRV upstream
$H_1 = H_{tank}$ $Q_1 = \dfrac{H_{tank} - C_{m,1}}{B_1}$	$H_m = C_{p,m} - B_1\,Q_m$ $Q_m = 0.5\,K_v{}^2\left(-(B_1 + B_2) + \sqrt{(B_1 + B_2)^2 - 4\,K_v{}^{-2}\left(C_{m,m+1} - C_{p,m}\right)}\right)$
PRV downstream	**Outlet orifice**
$H_{m+1} = C_{m,m+1} + B_2\,Q_{m+1}$ $Q_{m+1} = Q_m$	$H_n = C_{p,n} - B_2\,Q_n$ $Q_n = g\,A^2_{orifice}\left(-B_2 + \sqrt{B_2^2 - \frac{2}{g\,A^2_{orifice}}\left(z_n - C_{p,n}\right)}\right)$

4. On demand-driven and pressure-driven simulation

In a physical system, according to the Newton's second law of dynamics, the change of flow is a result of force (pressure) imbalance on both sides of a pipe. Hence, the flow (output) is a function of pressure (input). In a demand-driven simulation this causality is reversed, i.e. the flows are forced and the pressures are calculated such that in a physical pressure-driven system, the resulting flow would have been equal to the forced flow. The demand-driven approach has already been criticised, e.g. by Jung et al.[4], for overestimating the magnitude of pressure waves in the water-hammer model. This overestimation stems from the fact that in the demand-driven approach where flows are fixed, the produced pressure waves have no way to force additional amounts of water out of the system. Fixing water demands thus removes the causality between pressure and flow. From the control point of view (e.g. pressure management with PRVs) this lack of causality results in a non-physical model in which changes in valve position and thus head-drop across the valve have no effect on the flow. Thus, in order to correct the resulting pressure imbalance, all other pressures along the system are recalculated. In the rigid column model these changes are instantaneous since the pressure wave speed is infinite. The rigid column model is thus reduced to an algebraic system which means that the system's inertial term is neglected. The same applies to the water-hammer model in which the only dynamic effects, in absence of pressure dependent leakage, will stem from water compressibility and pipe elasticity. Since inertial dynamics are the most dominant slow dynamics in the transient flow and cannot be neglected, pressure-driven not demand-driven approach needs to be used for modelling pressure control systems such as PRVs.

5. Simulation results

In order to compare both models and assess their performance under a range of conditions and inputs, three simulation experiments were performed: 24-hr simulation with a diurnal demand profile capturing high and low flows (1); response to a ramp input in the orifice area (2); and response to step changes in the orifice area and PRV outlet pressure setpoint (3). By default, if not stated otherwise, the simulations were performed with the following parameters: L_1 = 10km, L_2 = 5km, $D_1 = D_2$ = 0.7m, $\lambda_1 = \lambda_2$ = 0.001, $a_1 = a_2$ = 1200m/s

5.1. Long-term simulation under diurnal demand profile

The 24-hr simulation under a diurnal demand profile provides information on the behaviour of both models under time-varying flow conditions. The diurnal demand profile is modelled with a time-varying orifice area, as shown in the top subfigure of Fig 3a. As predicted, the instability is triggered at low flow conditions when the gain margin becomes zero. We can see in Fig. 3a and, in more detail, in Fig. 3b, that the rigid column model approximates well the water-hammer model during stable operating conditions. However, the rigid column model cannot reproduce the oscillations predicted by the water-hammer model, nor can it predict when the PRV becomes unstable.

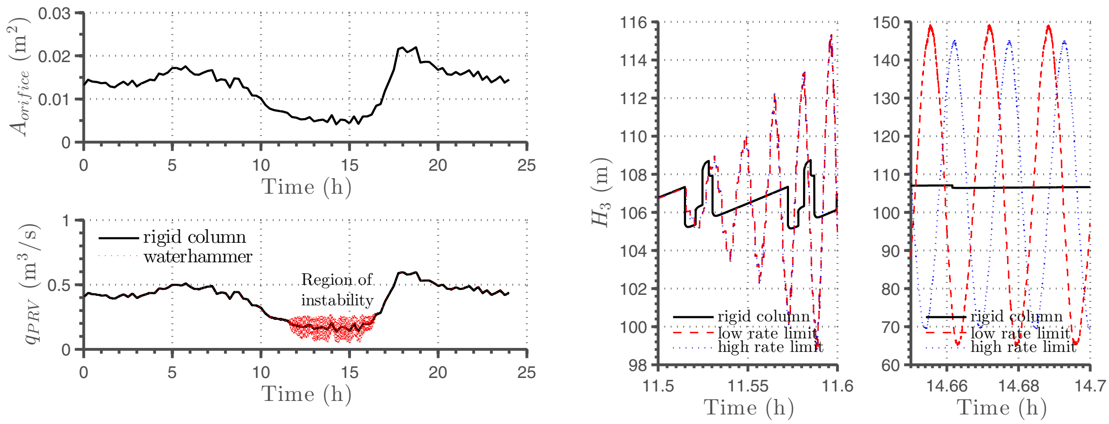

(a) (b)

Fig. 3: (a) Orifice area ($A_{orifice}$) and flow across the PRV (q_{PRV}) in a long-term simulation experiment (b) Downstream PRV head (H_3) at the onset (left) and during a fully established instability (right).

Fig. 3b shows the water-hammer model outputs with different valve opening/closing rate limits imposed on the actuator: the original ± 100/87 %/s (low rate limit) and ± 500/87 %/s (high rate limit). The left subplot of Fig. 3b demonstrates that the onset of instability is not influenced by the valve opening/closing rate. This suggests that the instability is not caused by a sudden large opening or closure in the valve caused by i.e. incoming pressure wave from an active element downstream or upstream in the network. Although such an event can in principle trigger an instability when the system is operating under a small gain margin, what we observe in the simulations here is a result of the intrinsic property of the PRV-WDN system itself. The pressure waves seem to be rather a result of instability than the cause of it. During a fully established instability the valve opening/closing rate does not seem to affect the pressure wave amplitude, only the phase-shift - see the right subfigure of Fig. 3b.

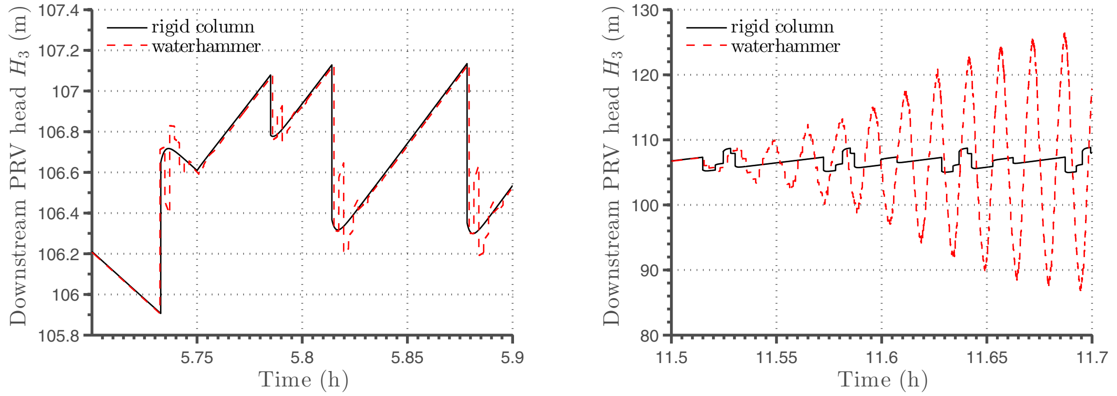

(a) (b)

Fig. 4: (a) Downstream PRV piezometric head (H_3) during stable conditions (b) Downstream PRV piezometric head (H_3) at the onset of instability.

The similarities and the differences between the water-hammer model and the rigid column model are better visualised in Fig 4. During stable conditions (Fig. 4a), the inertial rigid model follows closely the water-hammer model, whilst in an unstable region (Fig. 4b) the models diverge. This indicates that the fast pressure wave dynamics present in the water-hammer model but absent in the rigid column model are responsible for the transition from a stable to an unstable operating region.

5.2. Ramp input in the orifice area

Both models were additionally simulated under a gradually reducing orifice area leading to a reduction in flow and gradual closure of the valve element. This simulation scenario was designed to show that although instabilities can be triggered by events in the system if it happens to be operating close to instability, the instability can be induced under normal operation with smooth inputs when the gain of the closed-loop system becomes larger than the maximum stable gain. The simulations were performed for different integral time constants of the PID controller and different pipe lengths to show how these parameters affect the system stability. Fig. 5a shows that the instability is induced

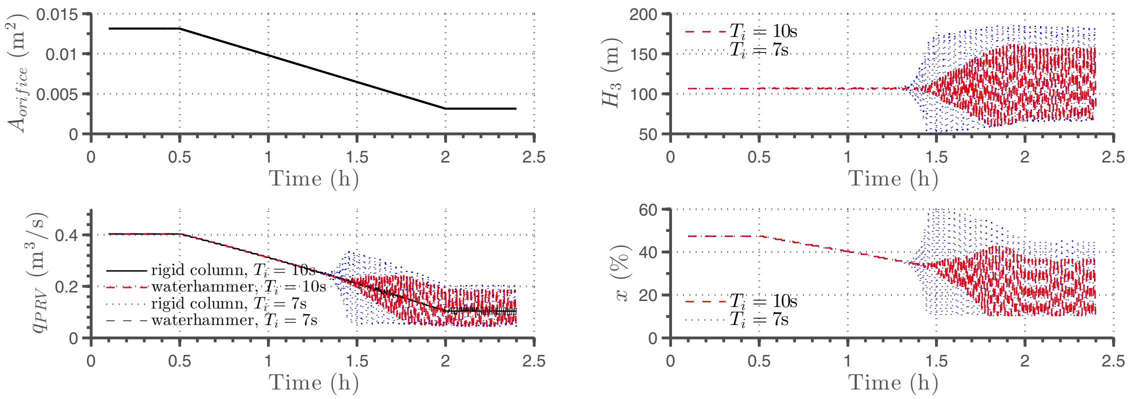

(a) (b)

Fig. 5: (a) Orifice area ($A_{orifice}$) and flow across the PRV (q_{PRV}) in a ramp-input experiment (b) Downstream PRV head (H_3) and valve position (x) in a ramp-input experiment.

in the system when $Q \approx 0.2\text{m}^3/\text{s}$ - the same value as in the diurnal flow simulation. Additionally, the instability is triggered earlier for lower integral time constant T_i, hence higher integral gain K_i. T_i does not only affect the moment of onset of instability but also the amplitude of oscillations - see Fig. 5b.

The system stability was also investigated as a function of the system inertia, i.e. the mass of water in the upstream and downstream pipes (Fig. 6). The inertial term in the system was halved by reducing the lengths of the pipes from $L_1 = 10$km to $L_2 = 5$km, and $L_1 = 5$km to $L_2 = 2.5$km. In order to maintain the same pressure losses and thus flow rates, the friction coefficients in the lower inertia system were increased from $\lambda_1 = \lambda_2 = 0.001$ to $\lambda_1 = \lambda_2 = 0.004$. Thus, the inertial term was reduced at the cost of increasing the dissipative friction forces.

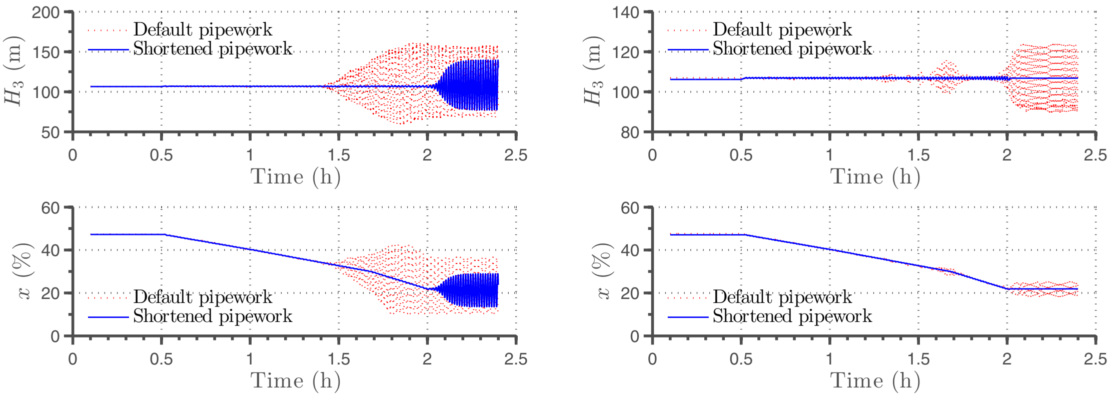

(a) (b)

Fig. 6: Development of instability in a ramp input experiment (a) Water-hammer model, $T_i = 10$s (b) Rigid column model, $T_i = 7$s.

Fig. 6a and Fig. 6b show the simulation results with the water-hammer model and the rigid column model respectively. The water-hammer model was simulated with $T_i = 10$s whilst for the rigid column model T_i was lowered to 7s in order to induce instability. As shown in Fig. 6 the instability is triggered later for the models with lower inertia and higher friction. From the system analysis point of view, inertia increases the model time constant τ, while friction increases damping ζ. Hence, the default model has slower dynamics but smaller damping of oscillations while the model with shorter pipes is faster but with higher damping. Whilst the exact relationship between inertia, friction and stability yet needs to be explored, we can now safely say that friction forces help remove instabilities by attenuating oscillations while inertia decreases the stability margin leading to slower responses in flow but higher responses in pressure. In the water-hammer model water kinetic energy is transformed into pressure upon valve opening/closure. The higher the inertia the higher the pressure, hence the amplitude of pressure waves is increased. In the rigid column model inertia only affects the, albeit stable, open-loop pole location $p = -1/\tau$. However as τ grows larger, the pole moves closer to zero hence closer to the unstable region. As shown in Fig. 6b instability can also be reproduced in the rigid column model although much later than in the water-hammer model and under lower T_i. This shows that the instability is a result of the properties of the PRV not the conditions in the WDN, although the fast dynamics associated with propagation of pressure waves have a decisive impact on the transition from stable to unstable behaviour.

5.3. Step input in the orifice area and PRV head setpoint

Dynamic responses to step changes in the orifice area and in the outlet PRV pressure setpoint were investigated to assess the system's disturbance rejection and setpoint tracking behaviour. The simulations were performed at two operating points: large initial orifice area $A_{orifice}^{init} = 0.0131\text{m}^2$ (Fig. 7a) and small initial orifice area $A_{orifice}^{init} = 0.008\text{m}^2$ (Fig. 7b). In the latter case the flows in the system are lower and hence the system is closer to instability. The simulations started with an upward step in $A_{orifice}$ of amplitude $\Delta A_{orifice} = 0.001\text{m}^2$ at 1000s followed by a downward step of the same amplitude at 2000s. Then an upward step of amplitude $\Delta H_{out}^{PRV,setpoint} = 10$m in the downstream head setpoint $H_{out}^{PRV,setpoint}$ at 5000s was followed by a downward step of the same amplitude at 6000s.

As can be seen in the top row of Fig. 7 a step change in orifice area results in an impulse-like response in the downstream head. Whilst in rigid column the change of head is almost instantaneous, the water-hammer model

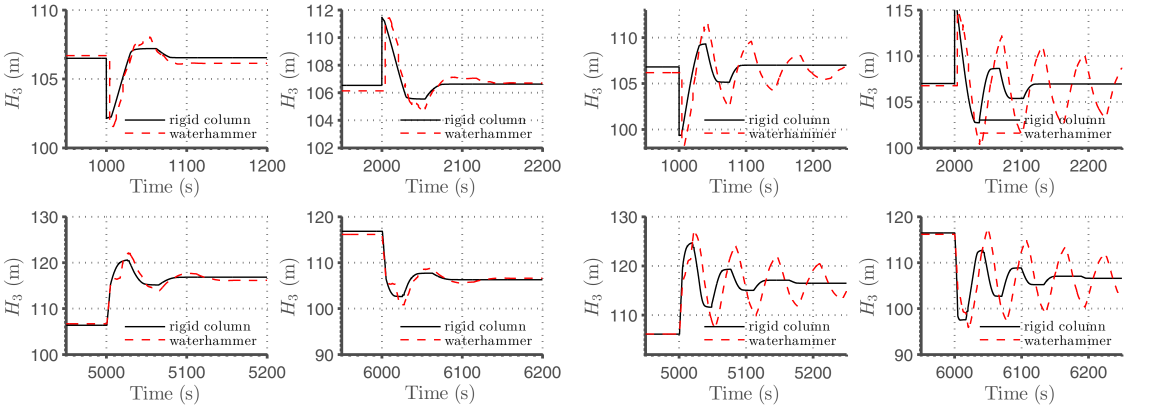

(a) (b)

Fig. 7: Responses to step changes in orifice area (top) and pressure head setpoint (bottom) at large valve openings (a) and low valve openings (b).

predicts a sightly more gradual change due to compressibility and elasticity effects. The step change in the pressure setpoint results, as expected, in a step-like response of the outlet pressure. The system responses are oscillatory with lower damping, higher overshoots and longer response times in Fig. 7b where the system is closer to instability. Additionally, as we get closer to an unstable operating point, we can see that the system's response to a downward step in orifice area is stronger than to an upward step (see top figures in Fig. 7b). The similarity between rigid column and water-hammer models deteriorates as we move away from normal operating conditions and into a less stable region where higher order (faster) dynamics associated with pressure waves become more dominant. This shows that the rigid column model can be used for designing PRV control schemes under stable operating conditions where the slower inertial dynamics dominate, but for the purpose of assessing the stability margins we need to identify these faster dynamics present in the water-hammer model. This will then allow us to create a lumped model for use in designing PRV controllers including both the disturbance rejection and the stability aspects.

6. Conclusions

In this paper we have shown that demand-driven modelling is not appropriate for the design and simulation of PRVs. Instead we should be using a pressure-driven approach. The rigid column model approximates well the water-hammer model under normal operating conditions but the models diverge when the system gets closer to an unstable operating point. The rigid column model can thus be used for designing PRV controllers, both with reference tracking and disturbance rejection aspects in mind, although only for stable operating conditions. Since the instabilities are triggered by faster pressure wave dynamics not present in the rigid column model, these dynamics need to be identified and incorporated into the lumped model in order to be able to assess the controller's stability margins and robustness. We have also shown how the network's properties such as inertia and friction affect the system's dynamics in both models but what remains to be done is to analyse how the network topology affects both the slow inertial dynamics playing part in disturbance rejection and the fast transient dynamics crucial for stability analysis.

References

[1] B. Ulanicki, P. Skworcow, Why PRVs tend to oscillate at low flows, Procedia Engineering (2014). 16th International Conference on Water Distribution System Analysis, WDSA2014.

[2] S. Prescott, B. Ulanicki, Dynamic modeling of pressure reducing valves, ASCE Journal of Hydraulic Engineering 129 (2003) 804–812.

[3] S. L. Prescott, B. Ulanicki, Improved control of pressure reducing valves in water distribution networks, Journal of Hydraulic Engineering 134 (2008) 56–65.

[4] B. B. S. Jung, P. F. Boulos, D. J. Wood, Effect of pressure-sensitive demand on surge analysis, American Water Works Association Journal (2009).